Multi-channel WDM RZ-to-NRZ format conversion at 50 Gbit/s based on single silicon microring resonator

Ding, Yunhong; Peucheret, Christophe; Pu, Minhao; Zsigri, Beata; Seoane, Jorge; Liu, Liu; Xu, Jing; Ou, Haiyan; Zhang, Xinliang; Hang, Dexiu

Published in:
Optics Express

Link to article, DOI:
10.1364/OE.18.021121

Publication date:
2010

Document Version
Publisher's PDF, also known as Version of record

Multi-channel WDM RZ-to-NRZ format conversion at 50 Gbit/s based on single silicon microring resonator

Yunhong Ding,[1,2,] Christophe Peucheret,[2] Minhao Pu,[2] Beata Zsigri,[2] Jorge Seoane,[2] Liu Liu,[2] Jing Xu,[2] Haiyan Ou,[2] Xinliang Zhang,[1] and Dexiu Huang[1,*]

[1]*Wuhan National Laboratory for Optoelectronics, School of Optoelectronics Science and Engineering, Huazhong University of Science and Technology, Wuhan, 430074, Hubei, China*

[2]*Department of Photonics Engineering, Technical University of Denmark, 2800 Kgs. Lyngby, Denmark*

[*]*wnlo2@mail.hust.edu.cn*

Abstract: We comprehensively analyze multiple WDM channels RZ-to-NRZ format conversion using a single microring resonator. The scheme relies on simultaneous suppression of the first order harmonic components in the spectra of all the RZ channels. An optimized silicon microring resonator with free spectral range of 100 GHz and Q value of 7900 is designed and fabricated for this purpose. Multi-channel RZ-to-NRZ format conversion is demonstrated experimentally at 50 Gbit/s for WDM channels with 200 GHz channel spacing using the fabricated device. Bit error rate (BER) measurements show very good conversion performances for the scheme.

OCIS codes: (060.2330) Fiber optics communications; (250.4745) Optical processing devices; (230.5750) Resonators; (130.3120) Integrated Optics devices.

References and links

1. Y. Yu, X. L. Zhang, J. B. Rosas-Fernández, D. X. Huang, R. V. Penty, and I. H. White, "Simultaneous multiple DWDM channel NRZ-to-RZ regenerative format conversion at 10 and 20 Gb/s," Opt. Express **17**(5), 3964–3969 (2009).
2. Y. Yu, X. L. Zhang, J. B. Rosas-Fernández, D. X. Huang, R. V. Penty, and I. H. White, "Single SOA based 16 DWDM channels all-optical NRZ-to-RZ format conversions with different duty cycles," Opt. Express **16**(20), 16166–16171 (2008).
3. Y. Yu, X. L. Zhang, D. X. Huang, L. J. Li, and W. Fu, "20-Gb/s All-optical format conversions from RZ signals with different duty cycles to NRZ signals," IEEE Photon. Technol. Lett. **19**(14), 1027–1029 (2007).
4. X. Lei, B. C. Wang, V. Baby, I. Glesk, and P. R. Prucnal, "All-optical data format conversion between RZ and NRZ based on a Mach-Zehnder interferometric wavelength converter," IEEE Photon. Technol. Lett. **15**(2), 308–310 (2003).
5. Y. Zhang, E. M. Xu, D. X. Huang, and X. L. Zhang, "All-optical format conversion from RZ to NRZ utilizing microfiber resonator," IEEE Photon. Technol. Lett. **21**(17), 1202–1204 (2009).
6. A. Yariv, "Universal relations for coupling of optical power between microresonators and dielectric waveguides," Electron. Lett. **36**(4), 321–322 (2000).
7. M. Popovic, "Theory and design of high-index-contrast microphotonic circuits," Ph.D. thesis (MIT, 2008).
8. Y. H. Ding, X. L. Zhang, and D. X. Huang, "Elastic polarization converter based on dual microring resonators," IEEE J. Quantum Electron. **45**(8), 1033–1038 (2009).
9. X. L. Cai, D. X. Huang, and X. L. Zhang, "Numerical analysis of polarization splitter based on vertically coupled microring resonator," Opt. Express **14**(23), 11304–11311 (2006).
10. F. P. Payne, and J. P. R. Lacey, "A theoretical analysis of scattering loss from planar optical waveguides," Opt. Quantum Electron. **26**(10), 977–986 (1994).
11. W. Y. Chen, R. Grover, T. A. Ibrahim, V. Van, W. N. Herman, P. T. Ho, T. A. Ibrahim, V. Van, W. N. Herman, and P.-T. Ho, "High-finesse laterally coupled single-mode benzocyclobutene microring resonators," IEEE Photon. Technol. Lett. **16**(2), 470–472 (2004).
12. Y. A. Vlasov, and S. J. McNab, "Losses in single-mode silicon-on-insulator strip waveguides and bends," Opt. Express **12**(8), 1622–1631 (2004).
13. R. Stoffer, K. R. Hiremath, M. Hammer, L. Prkna, and J. Ctyroky, "Cylindrical integrated optical microresonators: Modeling by 3-D vectorial coupled mode theory," Opt. Commun. **256**(1-3), 46–67 (2005).

#127740 - $15.00 USD Received 28 Apr 2010; revised 29 Jun 2010; accepted 7 Jul 2010; published 22 Sep 2010

1. Introduction

Optical format conversion is an important functionality in nodes interfacing optical networks operating with different modulation formats. Format conversion between return-to-zero (RZ) and non-return-to-zero (NRZ) on-off keying (OOK) formats is one essential conversion, since both formats are widely used in different parts of the networks [1]. In order to accommodate the growing demand of wavelength division multiplexing (WDM) networks, multi-channel format conversion is desired, because it will reduce the complexity, power consumption, and the cost of the optical networks. Recently, multiple channels dense WDM (DWDM) NRZ-to-RZ regenerative format conversion at 10 and 20 Gbit/s has been demonstrated using a single phase modulator (PM) and a fiber delay-interferometer (DI) [1,2]. RZ-to-NRZ format conversion has also been demonstrated for single channel using an optical fiber DI [3]. However, optical fiber DIs require phase tuning and stabilization, and integrated implementations would be preferred. A semiconductor optical amplifier (SOA) interferometic wavelength converter has also been applied for single channel RZ-to-NRZ format conversion [4], but the scheme is relatively complex, and the SOA will introduce extra power consumption. Recently, a new compact scheme based on an optical nano-fiber ring resonator has been demonstrated for single channel RZ-to-NRZ format conversion [5]. However, such a nano-fiber ring resonator is very sensitive to the surrounding environment, making it unstable. Currently, a simple compact and stable integrated scheme for simultaneous multiple WDM channels RZ-to-NRZ format conversion has still not been demonstrated.

In this paper, we theoretically analyze the performance of multi-channel RZ-to-NRZ format conversion at 50 Gbit/s based on a single microring resonator (MRR). Further, we experimentally demonstrate simultaneous four WDM channels RZ-to-NRZ format conversion at 50 Gbit/s based on a specially fabricated single silicon MRR. Bit error rates (BER) below 10^{-9} are realized for all four channels, and power penalty below 3 dB can be obtained. Due to its CMOS-compatible fabrication process, compact size for optical integration and stable operation, the proposed scheme is suitable for practical applications.

2. Principle

The method to realize format conversion from RZ to NRZ is based on optical spectrum transformation [3]. For a typical RZ format, as shown in Figs. 1(a) and 1(b), the optical spectrum contains very strong first harmonic components, as shown in Fig. 1(c). The method of optical spectrum transformation is to transform the RZ spectrum to a NRZ-like spectrum, as shown in Fig. 1(d), using periodic optical filters, such as fiber DIs or MRRs. The through transmission of the MRR can be expressed as [6]

$$t = \frac{r\left[1 - a\exp\left(-j\theta\right)\right]}{1 - ar^2\exp\left(-j\theta\right)} \tag{1}$$

where it is assumed that the MRR is geometrically symmetrical with identical through and drop coupling regions. r is the transmission coefficient of the coupling regions of the resonator. θ and a are the roundtrip phase shift and transmission coefficient along the ring waveguide, respectively. As shown in Fig. 1(c), the periodic notch filtering characteristic of the through transmission can be used to suppress the first order harmonic components of the RZ spectrum. Residual amplitude ripples in the converted NRZ signal, as shown in Fig. 1(e), can be further reduced by an additional optical bandpass filter (OBPF) [3]. The free spectral range (FSR) of the MRR should correspond to the frequency spacing between the two first order harmonic components in the spectrum of the RZ signal (corresponding to twice the bit rate of the signal). Thanks to the periodic nature of the through transmission of the MRR, simultaneous multiple WDM channels format conversion can be achieved by adopting a channel spacing equal to an integer (≥2) multiple of the FSR and tuning the MRR so that the

#127740 - $15.00 USD Received 28 Apr 2010; revised 29 Jun 2010; accepted 7 Jul 2010; published 22 Sep 2010

notches of the through transmission coincide with the first harmonic components of all channels. The residual intensity ripples can be suppressed for all channels using a wavelength demultiplexer such as an arrayed waveguide grating (AWG). Therefore multi-channel RZ-to-NRZ format conversion can be achieved, as shown in Figs. 1(f) and 1(g).

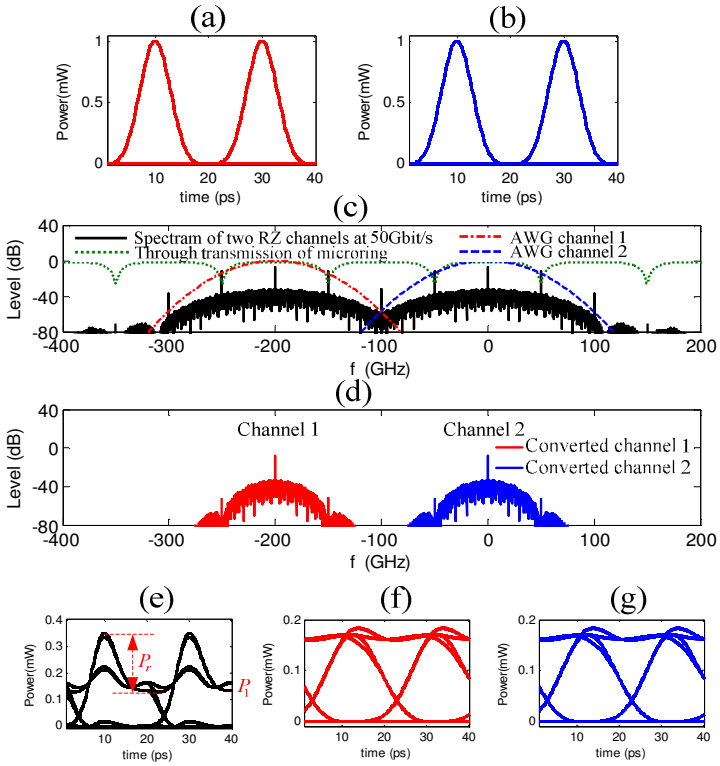

Fig. 1. Principle of the multi-channel RZ-to-NRZ format conversion, illustrated here for two channels. (a) and (b) show the eye diagrams of two different input RZ signals at 50 Gbit/s with 200 GHz channel spacing. (c) Spectrum transformation of the RZ-to-NRZ format conversion for the two channels utilizing the through transmission of the MRR. (d) Transformed converted NRZ spectra. (e) to (g) show the eye diagrams of the converted NRZ channels for single channel format conversion without AWG, as well as two channels operation after the MRR and ripples suppression by the AWG. In this illustration, $r^2 = 0.35$ **and** $a = 0.94$ for the MRR and the 3 dB bandwidth of the Gaussian AWG is 65 GHz.

The presence of amplitude ripples and pattern effects for the converted NRZ format impacts the performance of the format conversion [3]. Figures 2(a) and 2(b) analyze the Q factor and amplitude ripples of the converted NRZ signal for different Q values of the MRR and the OBPF 3 dB bandwidths at a bit-rate of 50 Gbit/s. The OBPF is modeled as a 1st order Gaussian type filter. The amplitude ripple is defined as the ratio between the maximum power deviation P_r and the average power of the high level P_1. For good format conversion, both high Q factor and low amplitude ripples are required for the converted signal. One can find that if the bandwidth of the filter is narrower than 50 GHz, the amplitude ripple of the converted NRZ signal is as low as 0.2, and independent of the Q value of the MRR (Fig. 2(b)). However, in this region, the Q factor of the converted NRZ signal is as low as 5 (Fig. 2(a)), which will lead to a poor bit error rate. The regions denoted by the white ellipses in Figs. 2(a) and 2(b) illustrate the optimized bandwidths of the OBPF and Q values of the MRR. A MRR with Q value around 8000, and an OBPF with a bandwidth around 65 GHz will result in the best RZ-to-NRZ format conversion with high Q factor and low amplitude ripples.

#127740 - $15.00 USD Received 28 Apr 2010; revised 29 Jun 2010; accepted 7 Jul 2010; published 22 Sep 2010

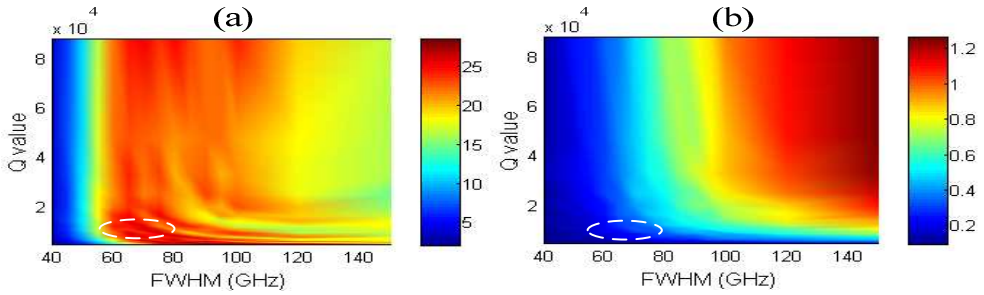

Fig. 2. (a) Q factor and (b) amplitude ripples of the converted NRZ signal versus Q value of the MRR and bandwidth of the OBPF for 50 Gbit/s format conversion.

In real applications, the exact location of the notches in the MRR through transmission will depend on temperature. The thermo-optical coefficient of silicon can be described by [7]

$$\frac{\Delta n(\Delta T)}{n(T_0)} \approx 0.01587\left(\frac{\Delta T}{T_0}\right) + 0.002392\left(\frac{\Delta T}{T_0}\right)^2 \qquad (2)$$

where $T_0 \approx 298.15K$ is the room temperature and $n(T_0) \approx 3.48$ is the silicon refractive index at room temperature. Δn is the deviation of the silicon refractive index induced by a temperature deviation ΔT. Such temperature-induced refractive index change will lead to a shift of the through transmission, hence to a frequency detuning Δf between the notches of the through transmission and the first harmonic components of the RZ spectrum, as shown in Fig. 3(a). Figure 3(b) illustrates the Q factor and amplitude ripples of the converted NRZ format as a function of the frequency detuning (or equivalent temperature deviation for a MRR with 100 GHz FSR) at optimum conditions (Q = 8000, FWHM = 65 GHz). One can find a frequency detuning tolerance of about 8 GHz (or equivalent temperature deviation tolerance of 0.8°C), where both the Q factor and amplitude ripples are not degraded noticeably. If the frequency detuning keeps increasing, the Q factor and amplitude ripples of the converted NRZ signal will be degraded significantly. This effect could be circumvented by temperature control of the chip.

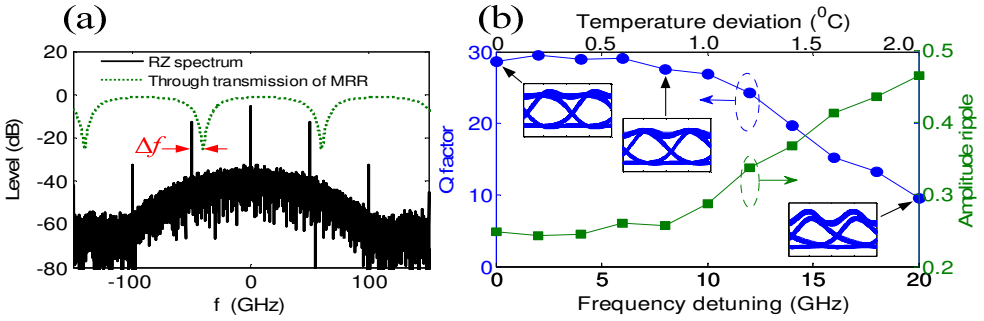

Fig. 3. (a) Illustration of the detuning between the notches of the through transmission and the first order harmonic components of the RZ spectrum. (b) Q factor and amplitude ripple of the converted NRZ signal as a function of frequency detuning Δf (or equivalent temperature deviation). Q = 8000, FWHM = 65 GHz.

3. MRR design and fabrication

3.1 Design

A silicon MRR with a FSR of 100 GHz and high extinction ratio is designed for RZ-to-NRZ format conversion at 50 Gbit/s. A silicon-on-insulator (SOI) wafer with top silicon layer of

#127740 - $15.00 USD Received 28 Apr 2010; revised 29 Jun 2010; accepted 7 Jul 2010; published 22 Sep 2010

250 nm is selected for the design. The cross section of the waveguide is designed as illustrated in Fig. 4(a). The waveguide width and height are designed to be 430 nm and 250 nm, respectively. A layer of benzocyclobutene (BCB) is used to cover the waveguide and form the upper cladding layer. A Ti heater is deposited on top of the BCB for thermally tuning the transmission of the MRR.

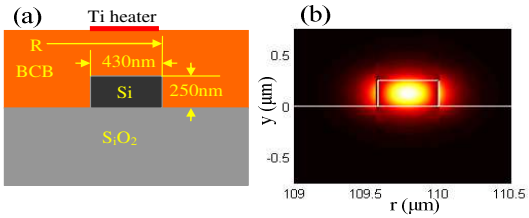

Fig. 4. (a) Cross section and (b) corresponding TE_0 mode profile of the electric field of the designed waveguide calculated by the full vectorial mode matching method [8,9].

To precisely design the FSR of the MRR, the group index of the waveguide should be calculated accurately. The wavelength dependence of the material refractive index of silicon is considered as follows [7]

$$n_{si}(\lambda) = 3.476\text{-}0.07805(\lambda\text{-}1.55)+0.082(\lambda\text{-}1.55)^2 \tag{3}$$

where λ is the wavelength. Figure 5(a) shows the effective index dispersion of the designed waveguide calculated by the full vectorial mode matching method (FVMM). The corresponding group index is estimated by $n_g = n_{eff}(\lambda) - \lambda \cdot \partial n_{eff}(\lambda)/\partial\lambda = 4.2971$ at 1550 nm. To obtain a FSR of 100 GHz around 1550 nm, the radius of the MRR should be 111 μm.

To obtain the target Q value and ER of the MRR, the scattering loss should also be estimated. The scattering loss can be simply evaluated by extending the 2D planar waveguide model [10] to 3D waveguide structures, and can be calculated as

$$\alpha = S\left(n_{core}^{\ 2} - n_{side}^{\ 2}\right)^2 \frac{k_0^{\ 3}}{4\pi n_{core}} \frac{\int_{inner-side} E^2 dy + \int_{outer-side} E^2 dy}{\iint E^2 da} \tag{4}$$

$$S = 2\sigma^2 L_c \int_0^{\pi} \frac{d\theta}{1 + L_c^{\ 2} k_0^{\ 2}\left(n_{eff} - n_{side}\cos\theta\right)^2} \tag{5}$$

where the two integrations in the numerator in Eq. (4) are along the inner and outer sides of the waveguide, respectively. The surface roughness is characterized by its roughness standard deviation σ and its correlation length L_c. n_{core}, n_{side} and n_{eff} are the refractive indices of the silicon core and BCB side cladding (taken equal to 1.56 according to [11]) and the effective mode refractive index, respectively. E is the mode profile of the electric field, as represented in Fig. 4(b), and $k_0 = 2\pi/\lambda$ is the wave number. With typical surface roughness parameters $\sigma = 2$ nm and $L_c = 50$ nm [12], a total propagation loss of 8.2 dB/cm is predicted for the TE_0 mode. Combined with the coupling coefficient calculated by the coupled mode theory (CMT) [8,13], the Q value of the designed MRR can be estimated. Figure 5(b) illustrates the calculated power coupling coefficient and estimated Q value as a function of the coupling gap of the MRR for TE_0 mode operation. According to the optimization of Sect. 2, a Q value around 8000 is preferred for our application. In consequence, a coupling gap of 180 nm is selected, corresponding to an estimated Q value of 8600 and an ER of about 20 dB.

#127740 - $15.00 USD Received 28 Apr 2010; revised 29 Jun 2010; accepted 7 Jul 2010; published 22 Sep 2010

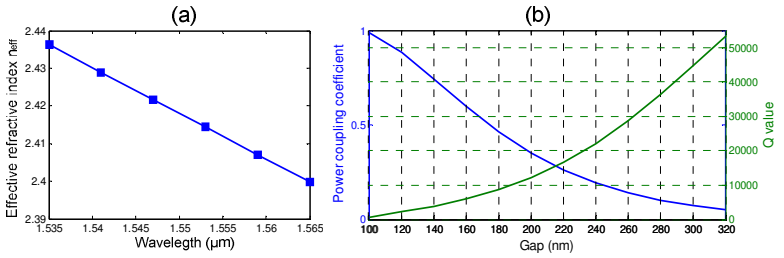

Fig. 5. (a) Calculated effective index dispersion of the designed waveguide for the TE_0 mode. (b) Calculated power coupling coefficient and Q value of the MRR as a function of the coupling gap for the TE_0 mode.

3.2 Fabrication and device characterization

The fabricated device is shown in Figs. 6 (a) and 6(b). It is fabricated on a SOI wafer with top silicon thickness of 250 nm and buried silicon dioxide of 3 μm. First, diluted (1:1 in anisole) electron-beam resist ZEP520A is spin-coated on the wafer to form a ~110 nm-thick mask layer. The MRR structure is then defined using electron-beam lithography (JEOL JBX-9300FS). After that, the sample is etched by inductively coupled plasma reactive ion etching (ICP-RIE) to transfer the patterns to the top silicon layer. A layer of 550 nm BCB is spin-coated afterwards as top cladding, and a layer of 400 nm ZEP520A is spin-coated in sequence as the mask layer for the micro heater. Electron-beam lithography is used again to define the patterns of the heater and pads. Finally, 100 nm thick titanium heater and pads are formed by evaporation and lift-off processes. The radius of the MRR is 110 μm, with the waveguide width of 435 nm and coupling gap of 178 nm for both through and drop coupling regions, as shown in Fig. 6(a). The output waveguide is tapered to 4 μm to increase the coupling efficiency to the lensed fiber. Figure 6(c) represents the measured transmission of the MRR. The ER of the transmission is as high as 20 dB, the measured FSR is 0.8 nm, corresponding to 100 GHz at 1550 nm, and the Q value is 7900, which all agree very well with our design target. The insertion loss of the device is about 16 dB, including the propagation loss in the silicon waveguide and the coupling loss between the lensed fibers and the device.

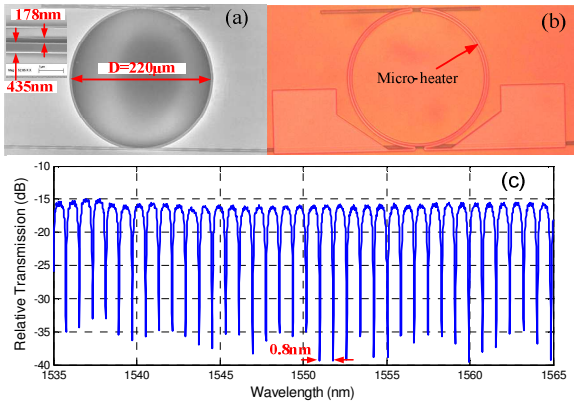

Fig. 6. (a) Scanning electron microscope (SEM) top view image of the fabricated device before BCB spinning. The inset is a close-up view of the coupling area between the ring and the straight waveguide. (b) Optical microscope picture of the fabricated device. The MRR is under the micro heater. (c) Measured transmission of the fabricated MRR.

4. Experiment and results

The experimental setup for WDM format conversion is represented in Fig. 7. Four channels of continuous wave (CW) laser light with wavelengths of 1548.16 nm, 1549.76 nm, 1551.36 nm,

#127740 - $15.00 USD Received 28 Apr 2010; revised 29 Jun 2010; accepted 7 Jul 2010; published 22 Sep 2010

and 1552.97 nm, respectively, are combined in a coupler, amplified by an erbium-doped fiber amplifier (EDFA), and simultaneously modulated at 50 Gbit/s in the 33% RZ-OOK format in two Mach-Zehnder modulators (MZMs), which are used as pulse carver (driven by a 25 GHz radio frequency clock) and data modulator, respectively. The four modulated RZ channels are amplified using a second EDFA to compensate for the modulators loss and further de-correlated by 50 m dispersion-compensating fiber (DCF) with total dispersion of −5.8 ps/nm at 1550 nm. Due to the high insertion loss of the device, the de-correlated multiple WDM RZ signal is amplified again by another EDFA. In order to ensure that all WDM channels are optimally coupled to the MRR, a polarization controller (PC) followed by a polarizer is first used to align all channels to the same polarization state. A second PC is then used to align the input polarization to the TE mode of the waveguide. The WDM RZ signal is then converted to a WDM NRZ signal by the MRR, and amplified by another EDFA afterward. Finally, the amplified converted WDM NRZ signal is wavelength demultiplexed by an AWG with channel spacing of 100 GHz and 3 dB bandwidth of 62 GHz, which is close to the optimum value of 65 GHz. The demultiplexed signal is finally detected in a preamplified receiver.

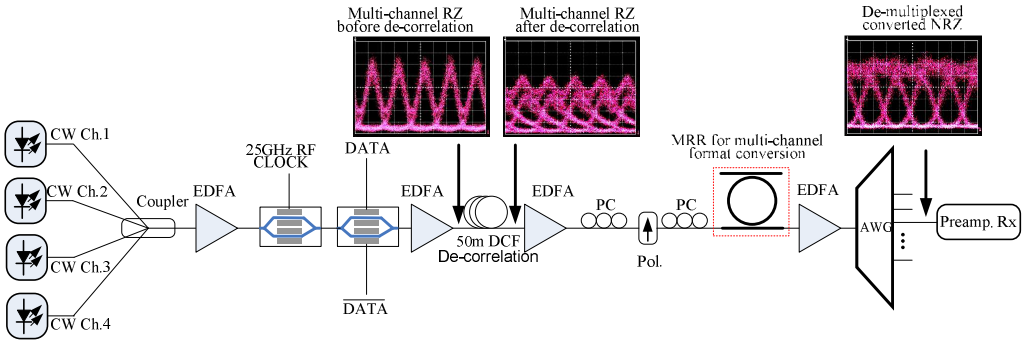

Fig. 7. Experimental setup for the multiple WDM channels RZ-to-NRZ format conversion.

4.1 Single channel operation

For single channel operation, channels 1, 3 and 4 are switched off, and only channel 2 at a wavelength of 1549.76 nm is switched on. The wavelength of channel 2 is fine tuned to align the two first order harmonic components of the RZ spectrum to the notches of the through transmission of the MRR. Figure 8(a) shows the spectrum transformation during the format conversion process. The first harmonics of the RZ spectrum are suppressed effectively by the MRR. The converted NRZ spectrum is very similar to that of an optical NRZ signal generated directly using a single MZM. The corresponding eye diagrams at the output of the RZ transmitter and of a NRZ modulated signal are also represented in Figs. 8(b) and 8(c) respectively. The RZ-to-NRZ format converted eye diagram (Fig. 8(d)) shows very little amplitude ripple and looks almost the same as the reference NRZ eye diagram (Fig. 8(c)). Figure 8(e) shows the BER measurement for single channel format conversion with a pseudorandom binary sequence (PRBS) length of 2^7-1. The power penalty (at a BER of 10^{-9}) of the converted NRZ signal at the MRR output is about 4 dB compared to the original RZ signal, while it is only 0.2 dB compared to the electrically generated NRZ reference signal. An extra power penalty of 1.3 dB is induced by the AWG.

#127740 - $15.00 USD Received 28 Apr 2010; revised 29 Jun 2010; accepted 7 Jul 2010; published 22 Sep 2010

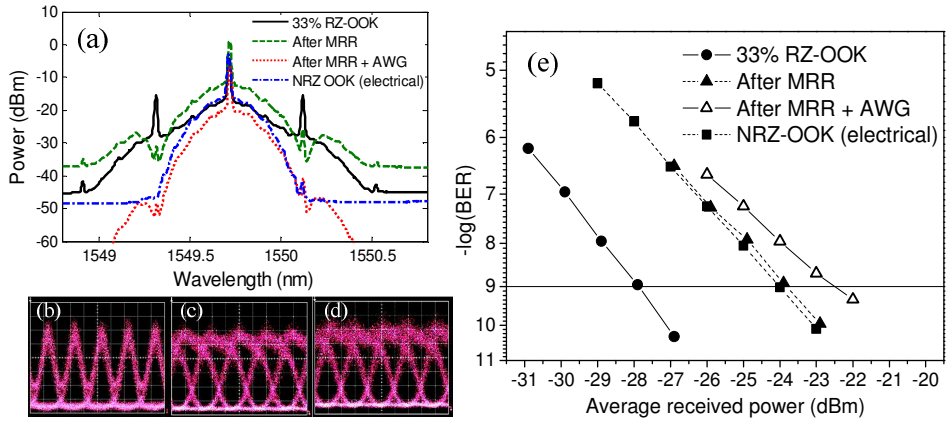

Fig. 8. (a) Spectra of the RZ signal at the transmitter and converted NRZ signals at the MRR and AWG outputs. The spectrum of a NRZ modulated signal is also shown as a reference. Eye diagrams of the input RZ (b), reference NRZ (c) and converted NRZ (d) signals. (e) BER measurements of the original RZ and of the converted NRZ signals after the MRR and the AWG, as well as of an electrically generated reference NRZ-OOK signal.

4.2 WDM operation

For WDM operation, all four channels are switched on. The wavelength of each channel is then fine tuned to align its first order harmonic components to the notches of the through transmission. Figures 9(a) and 9(b) illustrate the spectra of the WDM RZ and converted WDM NRZ signals, respectively. The first harmonic components of all four RZ channels are suppressed effectively, resulting in an effective spectrum transformation from WDM RZ to WDM NRZ. The AWG is used to demultiplex the converted WDM NRZ signal. The eye diagrams for WDM format conversion are represented in Fig. 10. The RZ signal (Fig. 10(a)) is first decorrelated by the DCF. Figure 10(b) shows the signal detected directly after the decorrelation DCF (without wavelength demultiplexing) when all four channels are present. The amount of dispersion of the decorrelation fiber is chosen such that the bit patterns of the four channels are no longer synchronized when they enter the MRR, while the introduced dispersion itself does not significantly degrade each channel, making dispersion compensation unnecessary after the MRR. After format conversion, very clear NRZ format eye diagrams are obtained for all four channels (Figs. 10(d)~10(g)), which are very close to the reference electrically modulated NRZ signal (Fig. 10(c)).

#127740 - $15.00 USD Received 28 Apr 2010; revised 29 Jun 2010; accepted 7 Jul 2010; published 22 Sep 2010

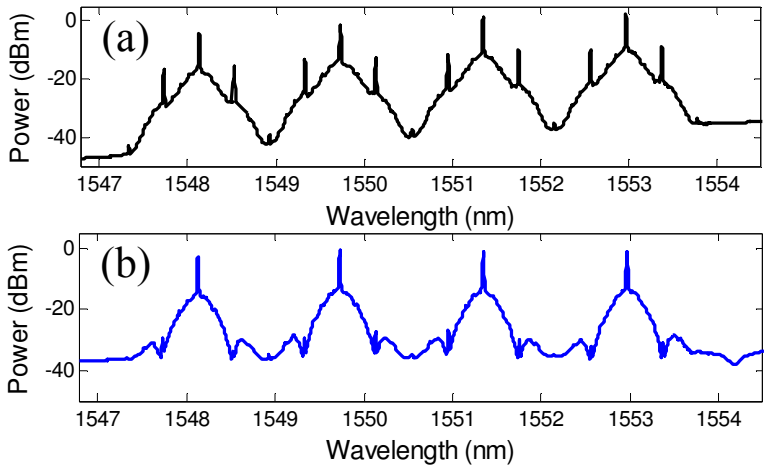

Fig. 9. Spectra of the four WDM channel signal. (a) WDM RZ signal. (b) Converted WDM NRZ signal.

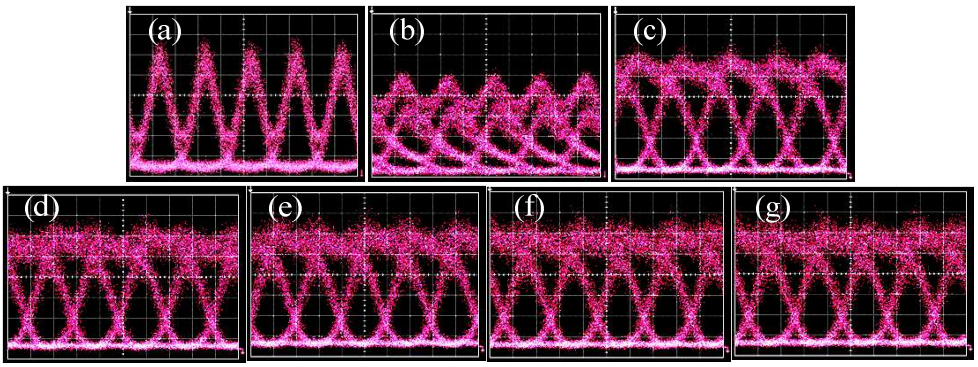

Fig. 10. Measured eye diagrams of (a) single RZ signal, (b) WDM RZ signals after decorrelation, (c) original reference NRZ signal, and (d)~(g) converted NRZ signals for channels 1 to 4.

Figures 11(a) and 11(b) show the results of BER measurements with a 2^7-1 PRBS for multiple WDM channels format conversion. BER values below 10^{-9} are obtained for all the four converted NRZ channels. Figures 11(c) and 11(d) show the corresponding power penalty at a BER of 10^{-9}. A power penalty of 2.5 to 3.5 dB is found for the RZ channels in the WDM configuration when only one channel is turned on compared to the single channel case without AWG. This penalty is attributed to strong filtering by the AWG demultiplxer. An extra penalty of 1.5 dB is measured in the WDM configuration when all channels are turned on. Crosstalk between the channels due to the fact that a passive coupler (therefore without filtering functionality) is used as wavelength multiplexer is believed to be responsible for this extra penalty (see Fig. 11(a)). For the converted NRZ signals, the measured power penalty is very low for channels 1~3 compared to the reference NRZ modulated signal for single channel operation. Further power penalties from 2 dB to 3 dB, which are caused by the crosstalk, are obtained for WDM channel operation. The power penalties for channels 2 and 3 are a little higher than channel 1, due to the difference in the number of directly adjacent channels. The BER performance is however somehow degraded for the fourth channel. It is speculated that a larger laser linewidth may be mostly responsible for this increased penalty after conversion to intensity noise by the MRR through transmission. Additionally, one can find that the power penalty is as high as 4.4 dB for the RZ signal of the fourth channel, which is the worst of the four channels (See Fig. 11(c)). This also leads to signal degradation for the

#127740 - $15.00 USD Received 28 Apr 2010; revised 29 Jun 2010; accepted 7 Jul 2010; published 22 Sep 2010

fourth converted NRZ signal for both single and WDM channel operation. However, the power penalty could be improved by using a real multiplexer, instead of a coupler, to multiplex the different channels and reduce the crosstalk. Improving the insertion loss of the MRR can also improve the power penalty thanks to an expected reduction of the induced optical signal-to-noise ratio (OSNR) degradation.

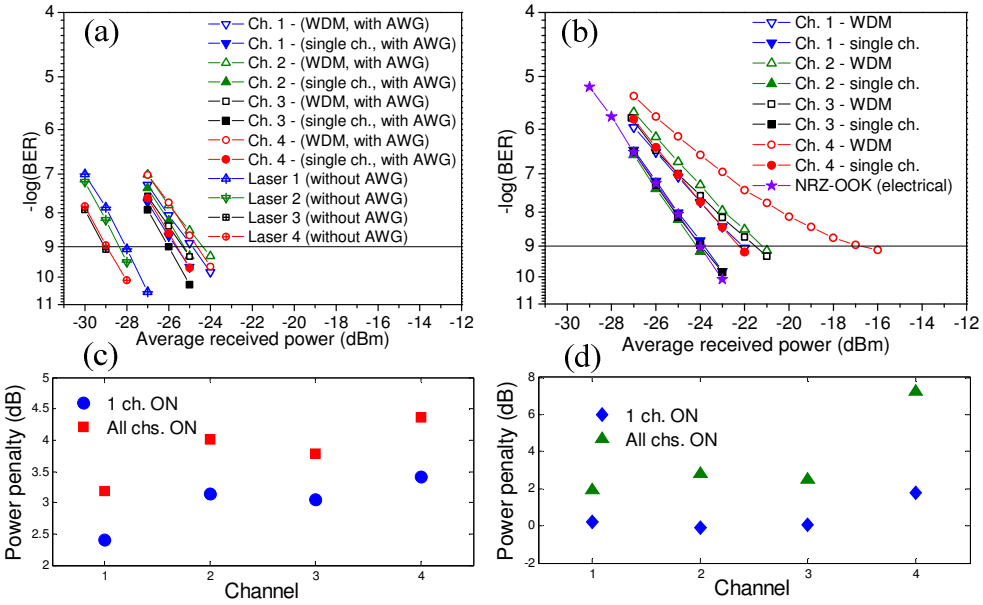

Fig. 11. (a) Back-to-back BER measurement of the RZ channels (single channel operation, with and without AWG, as well as WDM operation) (b) BER measurement of the converted NRZ channels in single channel and WDM operation, as well as an electrically generated reference NRZ signal. (c) Power penalties of the RZ signal output from the AWG for single and multiple WDM channels cases, compared to the original RZ signals without AWG. (d) Power penalty of the output converted NRZ signal for single and multiple WDM channels cases, compared to the reference electrically modulated NRZ signal. Power penalties are measured at BER of 10^{-9}.

5. Conclusion

We have comprehensively analyzed, and further demonstrated both single and multiple WDM channels RZ-to-NRZ format conversion at 50 Gbit/s utilizing a single silicon MRR with FSR of 100 GHz and Q value of 7900. Bit error measurements show the very good performance of the scheme. Due to its CMOS-compatible fabrication process, our scheme is very promising for practical implementations.

Acknowledgement

This research was sponsored by the National Natural Science Foundation of China (Grant No. 60577007), the National Basic Research Program of China (Grant No. 2006CB302805), and the Program for New Century Excellent Talents in University of Ministry of Education of China (Grant No. NCET-04-0715). Yunhong Ding would like to thank the support of the Chinese Scholar Council (CSC). Support from the Villum Kann Rasmussen foundation through the Nanophotonics for Terabit Communications (NATEC) centre of excellence is acknowledged.